Scientific Research Publishing

Journal of Geoscience and Environment Protection, 2021, 9, 144-157
https://www.scirp.org/journal/gep
ISSN Online: 2327-4344
ISSN Print: 2327-4336

Mapping Subsurface Seepage Flow Patterns in Proximity to a Coal Combustion Residual Landfill Using Electrical Resistivity Tomography

Ruobai Zhao[1*], Neil Anderson[1], David Rogers[1], Evgeniy Torgashov[1], Jing Sun[2]

[1]Department of Geosciences and Geological and Petroleum Engineering, Missouri University of Science and Technology, Rolla, USA
[2]Department of Mathematics and Statistics, Missouri University of Science and Technology, Rolla, USA
Email: *rzmqc@mst.edu

How to cite this paper: Zhao, R. B., Anderson, N., Rogers, D., Torgashov, E., & Sun, J. (2021). Mapping Subsurface Seepage Flow Patterns in Proximity to a Coal Combustion Residual Landfill Using Electrical Resistivity Tomography. *Journal of Geoscience and Environment Protection, 9,* 144-157.
https://doi.org/10.4236/gep.2021.92009

Received: January 22, 2021
Accepted: February 21, 2021
Published: February 24, 2021

Abstract

Electrical resistivity tomography data were acquired in proximity to the coal combustion residual landfill in an effort to image and analyze seepage pathways through the shallow residual soil and underlying karsted limestone bedrock. The water table is at a depth of more than 45 m. The most prominent subsurface seepage pathways identified on the acquired electrical resistivity tomography data are located immediately adjacent to the toe of the landfill and are attributed to stormwater run-off. The moisture content of the limestone appears to decrease gradually with increasing distance from the toe of the landfill, suggesting there is also a horizontal component of moisture flow in the subsurface. Shallow limestone with higher moisture content generally underlies or is in close proximity to anthropogenic features such as drainage ditches and clay berms that are designed to channel run-off. At one location, electrical resistivity tomography data were acquired along essentially the same traverse at different times of the year, and the resistivity of shallow limestone overall was lower on the data acquired after heavy rains.

Keywords

Coal Ash, Electrical Resistivity Tomography (ERT), Seepage, Solid Waste Landfill, Geophysical Methods, Coal Combustion Residual (CCR)

1. Introduction

Coal combustion residual (CCR) landfills are dry storages of coal ash produced in the coal combustion process. The safe disposal and containment of CCR landfills were addressed by the U.S. Environment Protection Agency (EPA) CCR rule in 2015. As part of the minimum criteria, the successful containment of CCR landfills requires a properly designed and constructed run-on/run-off control system to prevent groundwater contamination (US EPA, 2015).

A run-on control system is designed to prevent tributary accretion flowing onto the active portion of CCR landfill, normally by constructing drainage ditches and diverting berms to channel away incoming flow when natural drainage of run-on is not available. A Run-off control system is designed to drain and collect direct precipitation (e.g., rainfall, melting snow) that falls onto the CCR landfill.

When a CCR landfill (or part of the landfill) ceases operation, a "cap cover" (typically a vegetative soil layer overlying a low permeability liner) is placed on top to minimize run-off infiltration into the CCR deposit. Cap cover components can vary from site to site, depending on the location of the landfill and then-effective regulations governing the design criteria (Zhao et al., 2020).

Preferably, the surface of the CCR landfill slopes with a narrow crown, which allows most of the run-off to flow down along the flanks of the CCR landfill. The perimeter berms and drainage ditches then channel run-off into a stormwater retention pond. In places where run-off tends to accumulate, such as at the toe of the landfill and in drainage ditches, moisture can seep into the subsurface, especially where bedrock is pervasively fractured and overlain by weathered permeable soil (e.g., in karst terrain) (**Figure 1**).

This study was conducted to identify and map seepage flow patterns in close proximity to a CCR landfill. The electrical resistivity tomography (ERT) data presented in this study were acquired as part of a groundwater monitoring effort. The results presented provide insight into a cost-effective investigation method for landfill seepage analysis.

2. Site Geology

The target CCR landfill site locates in southwest Missouri, USA (**Figure 2**), and is situated on the Springfield Plateau, where land is underlain by Paleozoic carbonate rocks that are susceptible to karstification.

The local bedrock is comprised of Mississippian limestones that are mainly limestones with intercalated beds of chert and impure flint, and some sandstones and shales (Shepard, 1898). The uppermost and surface bedrock unit is the Osagean series Burlington-Keokuk limestone, which is susceptible to karstification. The Burlington-Keokuk limestone is overlain by unconsolidated residual materials that comprise red clay, silt, and rock fragments as a result of bedrock weathering (Vandike & Sherman, 1994). Under the Burlington-Keokuk limestone are the Elsey and Reeds-Spring limestone, which comprises of Osagean series carbonates and cherty carbonates and are underlain by the Pierson Formation.

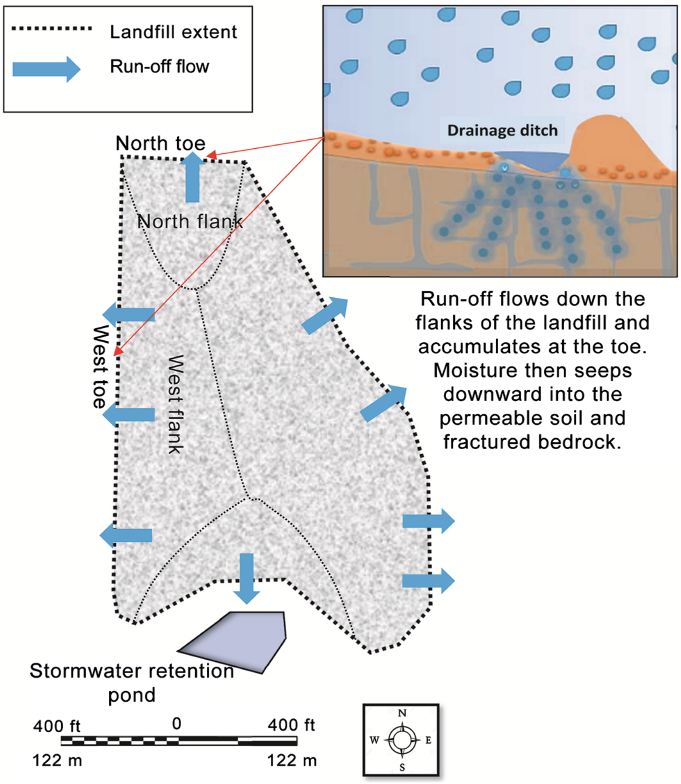

Figure 1. Sketch of a CCR landfill (aerial view). Stormwater run-off mostly flows down along the flanks of the landfill and temporarily accumulates at the toe and seeps downward into the permeable soil and fractured bedrock.

System	Series	Formation	Thickness (ft)	Thickness (m)
Mississippian	Osagean	Burlington-Keokuk Formation	155-270	47.2-82.2
		Elsey Formation	25-75	7.6-22.9
		Reeds-Spring Formation	0-125	0-38.1
		Pierson Formation	5-90	1.5-27.4

Figure 2. The study area is underlain by Mississippian limestones and the upper bedrocks are predominantly pervasively fractured Burlington-Keokuk Formation limestone (Vandike, 1993).

3. Data Acquisition

In this study, a total of seven ERT profiles were acquired in proximity to the

CCR landfill. The primary equipment included an automated 8-channel resistivity meter AGI SuperStingR8 system (**Figure 3**), several deep-cycle marine batteries, two switch boxes, multiple ERT cables with electrodes attached, a large number of stainless-steel stakes and a laptop for data transfer and field-processing (Zhao & Anderson, 2018). A 5 ft (1.52 m) electrode spacing, and a dipole-dipole array were used. The dipole-dipole array is sensitive to horizontal changes in resistivity, and works well for mapping vertical structures, such as solution-widened joints and cavities (Loke, 2018). Investigation depth is on the order of 100 ft (30.48 m).

Borehole control data and MASW (multichannel analysis of surface waves) control data were also acquired (Zhao, 2018). Additionally, more than fifty ERT profiles were acquired significant distances away from the CCR landfill in the general study area. These control data are not presented in this paper.

As shown in **Figure 4**, ERT profiles 1 and 2 were acquired along north-south oriented ERT traverses with a 60 ft (18.3 m) interval, in close proximity to the west toe of the landfill. At a different time of year, ERT profiles 3, 4, 5 were acquired at 20 ft (6.1 m) intervals along north-south oriented ERT traverses, progressively further away from the west toe of the landfill. ERT profile 6 was acquired along a west-east oriented ERT traverse, in close proximity to the north toe of the landfill. At a different time of year, ERT profile 6A was acquired essentially along the same traverse as profile 6.

4. Data Processing

Field ERT data acquired at the site were processed using a software Geotomo Res2DInv (Loke, 2018). The field ERT data were recorded as apparent resistivity values and then inverted into a 2-D resistivity model of the subsurface.

The processing includes subdividing the model (vertical cross-section) into multiple number of model blocks, generating a synthetic model with apparent resistivity values of the model blocks matching the field apparent resistivity values

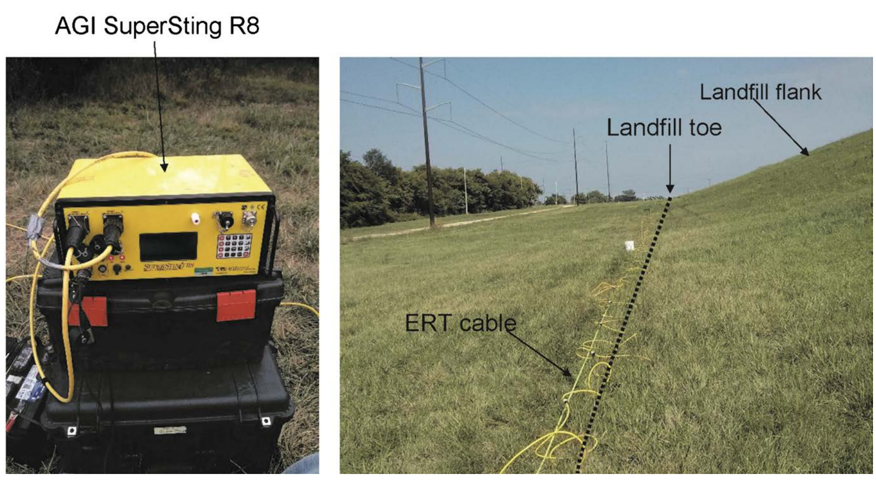

Figure 3. ERT data acquisition at the toe of the CCR landfill using an automated multi-electrode AGI SuperSting R8 system.

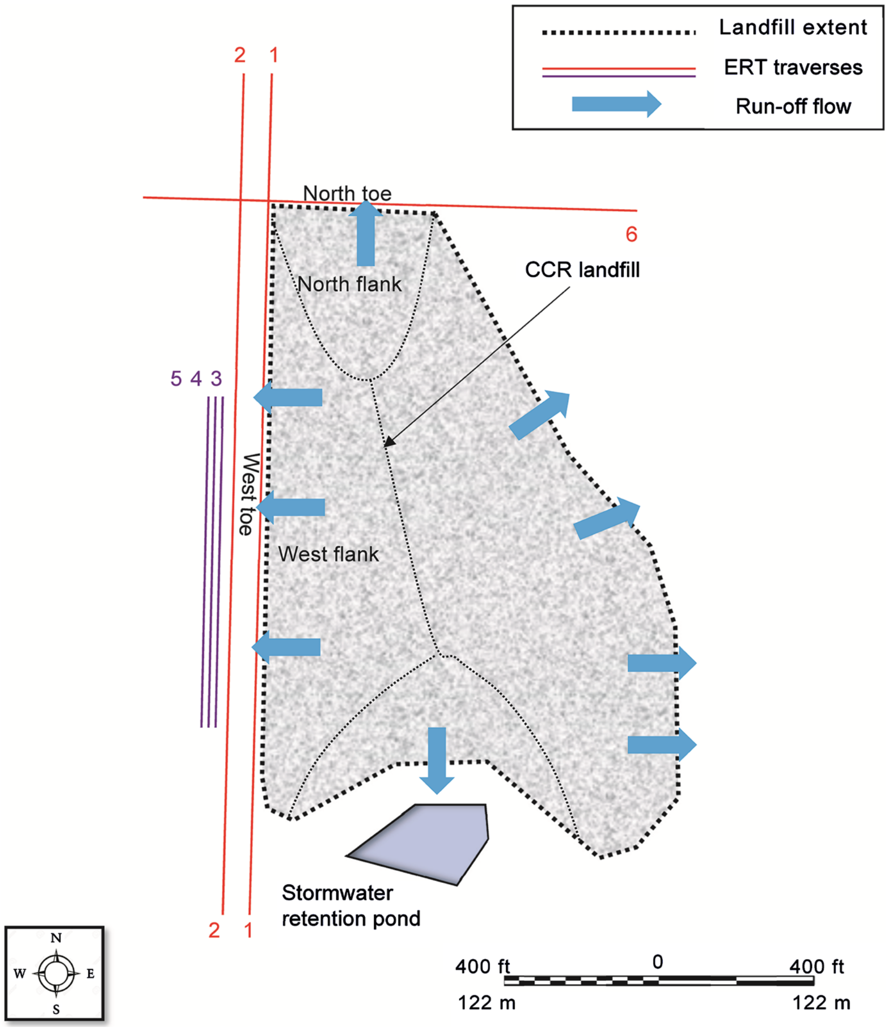

Figure 4. Sketch of the CCR landfill (aerial view) of locations of the ERT traverses. The ERT profiles were acquired in proximity to the north toe and south toe of the landfill.

as close as possible, and generating a 2-D resistivity model, using a finite-element modeling (if elevation control is present!) subroutine and a L1 norm method ("robust data constraint") inversion method (Claerbout and Muir, 1973). The L1 norm method ("robust data constraint") inversion method is more appropriate than a non-linear smoothness-constrained least-squares optimization technique (DeGroot-Hedlin and Constable, 1990; Sasaki, 1992; Loke et al., 2003) in karst terrain, as sharp interfaces between different regions with different resistivity values are present.

5. Results and Discussion

It is important to note that even a thin film of moisture on the soil grain could transmit significant current. Generally, soil and rock with higher moisture content are characterized by lower resistivity values compared to soil and rock with lower moisture content. Rock is generally less porous than soil, therefore, it is generally characterized by higher resistivity values than overlying soil.

In this study, the "top-of-rock" (soil-rock contact) was difficult to confidently map in places on the ERT profiles where shallow bedrock was pervasively fractured and moist from run-off, and hence was characterized by resistivity values comparable to that of overlying permeable and moist soil.

As mentioned previously, more than fifty ERT profiles (not shown in this study) were acquired elsewhere in the greater study area. The "top-of-rock" was readily identified on these ERT profiles and generally correlates well with the 125 ohm-m resistivity contour interval and is consistent with borehole control and MASW (multichannel analysis of surface waves) control (Kidanu et al., 2016).

Herein, soil that has resistivity values higher than 125 ohm-m will be interpreted as "dry soil", soil that has resistivity values less than 125 ohm-m will be interpreted as "moist soil". Bedrock that has resistivity values greater than 900 ohm-m will be interpreted as "dry bedrock", bedrock that has resistivity values from 125 ohm-m to 900 ohm-m will be interpreted as "moist bedrock", and bedrock that has resistivity values less than 125 ohm-m will be interpreted as "very moist bedrock".

5.1. ERT Profile 1 and ERT Profile 2

As shown in **Figure 5**, ERT profile 1 was acquired immediately adjacent to the west toe of the landfill. ERT profile 2 was acquired 60 ft (18.3 m) to the west of ERT profile 1, further away from the CCR landfill.

Processed ERT profile 1 and ERT profile 2 are 2-D resistivity images of the subsurface directly underneath ERT traverse 1 and ERT traverse 2, respectively. As shown in **Figure 6**, interpreted top-of-rock (soil-rock contact) is highlighted in black. The soil layer is interpreted as approximately 20 ft (6.1 m) thick, which is consistent with boring control, MASW (multichannel analysis of surface waves) control and ERT control acquired elsewhere in the greater study area.

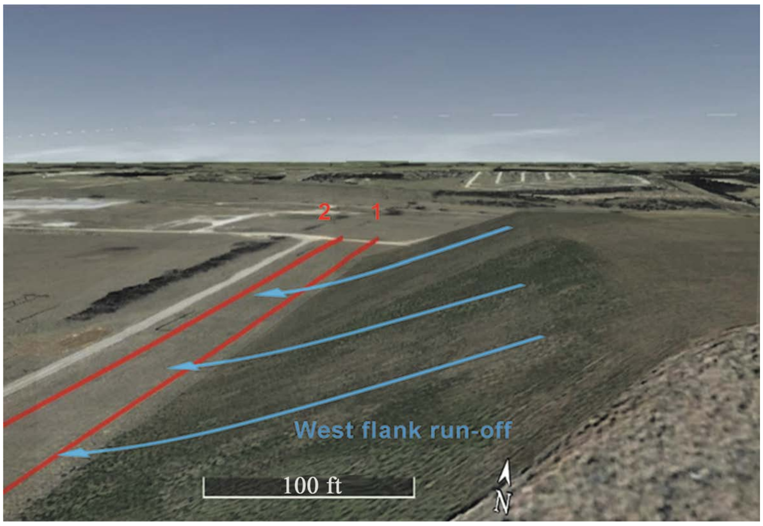

Figure 5. ERT profile 1 and ERT profile 2 (red lines) were acquired at the west toe of the landfill along N-S oriented traverses.

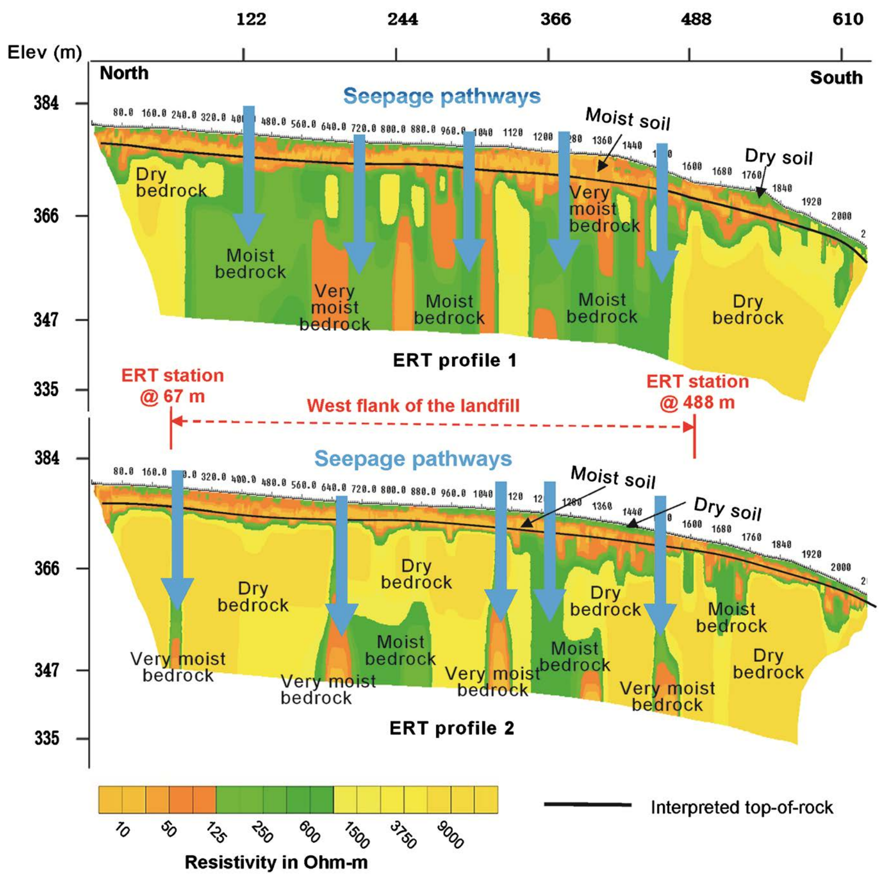

Figure 6. Interpreted ERT profile 1 (upper) and ERT profile 2 (lower). The vertical axis is elevation above mean sea level in meters, the horizontal axis is the length of the ERT traverse in meters.

The soil is classified as dry soil (resistivities > 125 ohm-m) and moist soil (resistivities < 125 ohm-m). Generally, dry soils overly moist soils.

Interpreted top of bedrock is approximately 20 ft (6.1 m) below the ground surface. The bedrock is classified as dry bedrock (resistivities > 900 ohm-m), moist bedrock (125 ohm-m < resistivities < 900 ohm-m), and very moist bedrock (resistivities < 125 ohm-m). Generally, shallow bedrocks are very moist and they overly moist bedrocks and dry bedrocks.

The west flank of the CCR landfill lies between ERT stations at 67 m and 488 m. Within this range, the bedrock in ERT profile 1 is mostly characterized by very moist bedrock (resistivities < 125 ohm-m) and moist bedrock (125 ohm-m < resistivities < 900 ohm-m), indicating moisture has seeped through overlying permeable soil into the pervasively fractured Burlington-Keokuk limestone. It appears that run-off flowing down the west flank of the CCR landfill accumulated at the toe and seeped into the subsurface.

Within the same range (between ERT stations 67 and 488), the bedrock on ERT profile 2 is mostly characterized by dry bedrock (resistivities > 900 ohm-m). Very moist bedrock and moist bedrock are present but to a less extent as compared to ERT profile 1, which indicates less moisture has seeped through overlying permeable soil, into the pervasively fractured Burlington-Keokuk limestone.

Visual analysis of the resistivity patterns of ERT profile 1 and ERT profile 2 also suggests that moisture seeped through the subsurface along near vertical seepage pathways (highlighted in blue arrows). Moisture content is the greatest in the bedrock immediately adjacent to the landfill toe, and gradually decreases as distance to the toe increases, indicating that there also appears to be a lateral component to seepage away from the landfill.

5.2. ERT Profiles 3, 4 and 5

In proximity to the west toe of the landfill, but at a different time of year, ERT profiles 3, 4, 5 were acquired with 20 ft (6.096 m) intervals (**Figure 7**). A clay berm that was constructed to divert surface run-off is present at the survey location.

The resistivity patterns shown on ERT profiles 3, 4, 5 (**Figure 8**) suggests that the shallow bedrock characterized by very moist bedrock (resistivities < 125 ohm-m) and moist bedrock (125 ohm-m < resistivities < 900 ohm-m) generally underlies the clay berm. Taking into consideration the location of the clay berm, and surface run-off drainage patterns, it appears that run-off flowing down from the west flank of the landfill has been intercepted by the clay berm, accumulated temporarily and caused moisture to seep through overlying permeable soil, into the pervasively fractured Burlington-Keokuk limestone.

Visual analysis of resistivity patterns of ERT profiles 3, 4 and 5 also suggests that moisture seeped through the subsurface along near vertical seepage pathways (highlighted in blue arrows). Among the three ERT profiles, the seepage volume is the greatest on ERT profile 3, which was acquired the closest to the landfill toe, and the least on ERT profile 5, which was acquired furthest away from the landfill toe. Moisture content in the bedrock decreases with increasing distance from the landfill toe, indicating there also appears to be a lateral component to

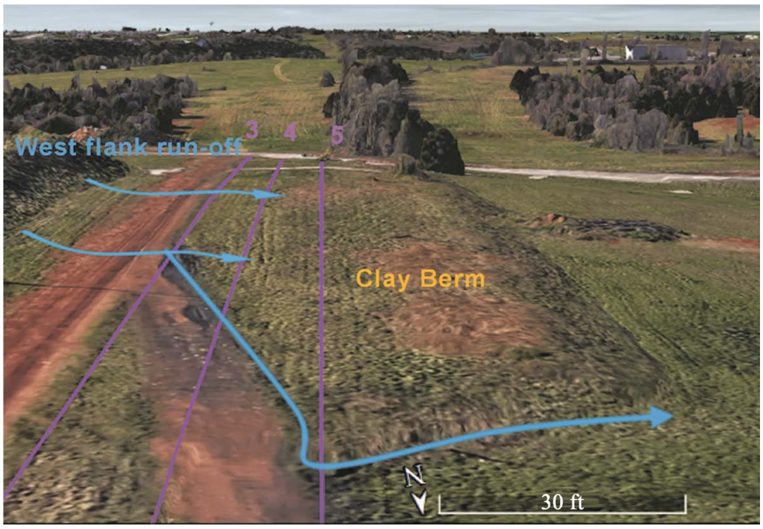

Figure 7. ERT profiles 3, 4 and 5 (purple lines) were acquired in proximity to the west toe of the landfill along N-S oriented traverses. A man-made clay berm is present at this location and underlies the ERT traverses.

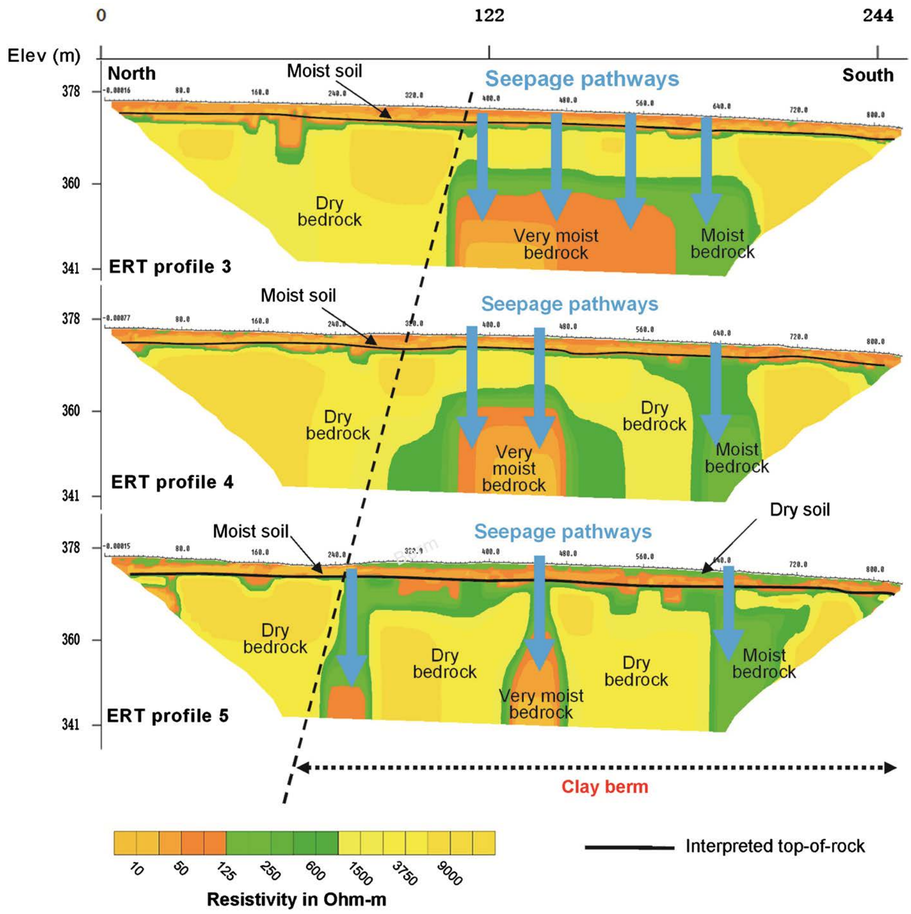

Figure 8. Interpreted ERT profile 3 (upper) and ERT profile 4 (middle) and ERT profile 5 (lower). The vertical axis is elevation above mean sea level in meters, the horizontal axis is the length of the ERT traverse in meters.

seepage away from the landfill. These findings are consistent with and support the interpretations of ERT profile 1 and ERT profile 2.

5.3. ERT Profile 6

ERT profile 6 was acquired immediately adjacent to the north toe of the landfill, as shown in Figure 9.

The north flank of the CCR landfill lies between ERT stations at 85 m and 219 m. Within this range, the subsurface bedrock is mostly characterized by moist bedrock (125 ohm-m < resistivities < 900 ohm-m), indicating moisture has seeped through overlying permeable soil, into the pervasively fractured Burlington-Keokuk limestone. This is attributed to run-off from the north flank of the CCR landfill, accumulating at the toe and seeping downward.

Additionally, the presence of anthropogenic features appears to be the cause of locally higher bedrock moisture content. As shown in Figure 10, a north-south oriented drainage ditch constructed by the roadway intercepts ERT traverse 6 at station 61, and the subsurface bedrock directly underneath is mostly characterized by moist bedrock (125 ohm-m < resistivities < 900 ohm-m), indicating

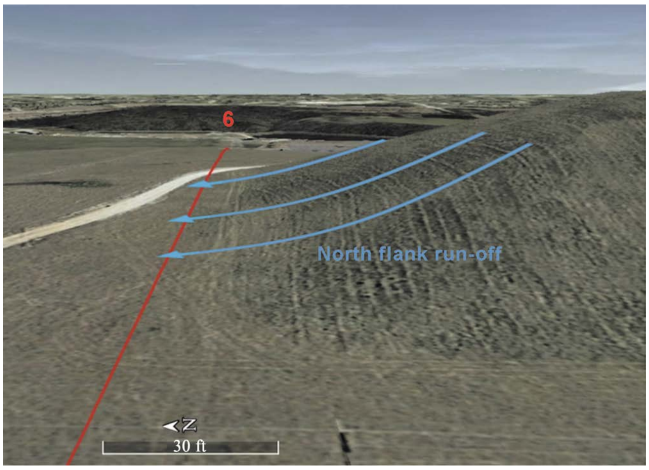

Figure 9. ERT profile 6 (red line) was acquired immediately adjacent to the north toe of the CCR landfill.

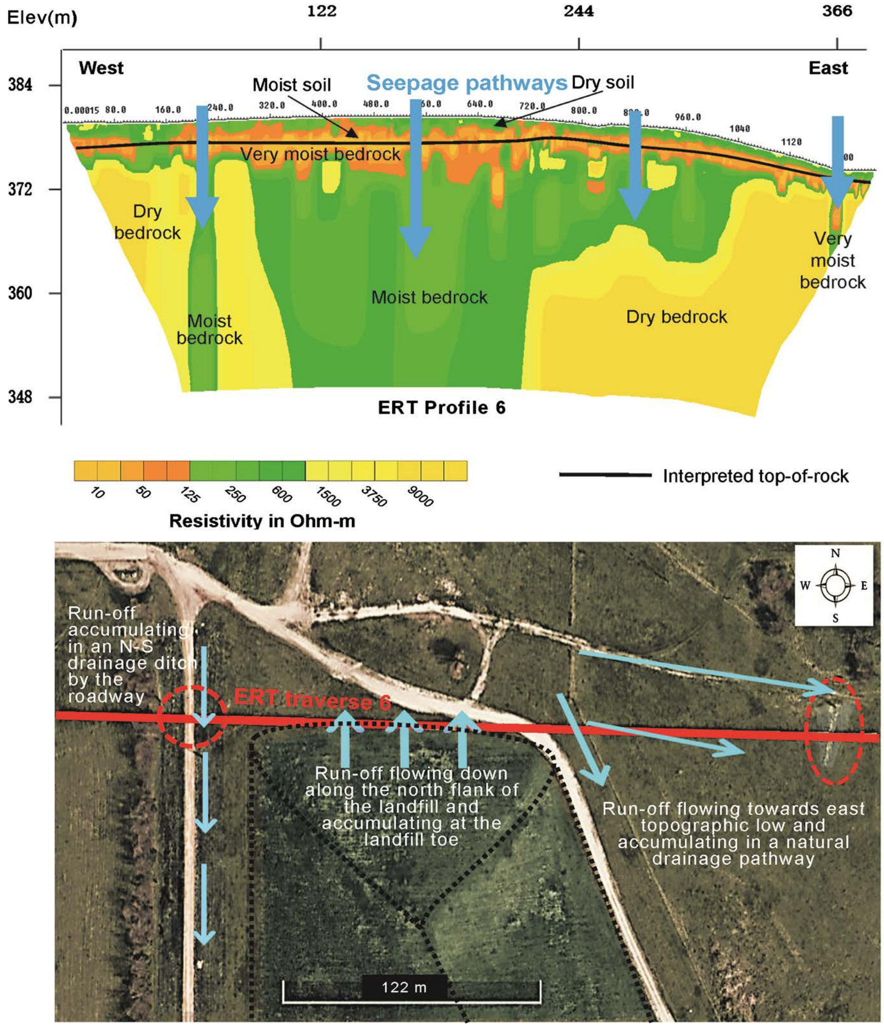

Figure 10. Interpreted ERT profile 6 (upper) and corresponding Google Earth image (lower) of the west of the landfill showing the ERT traverse and anthropogenic features. The vertical axis is elevation above mean sea level in meters, the horizontal axis is the length of the ERT traverse in meters.

concentrated run-off flowing along the north-south oriented drainage ditch has seeped down into the subsurface. Similarly, underneath ERT station 366, bedrock is mostly characterized by very moist bedrock (resistivities < 125 ohm-m), which is attributed to run-off concentrating in a natural drainage pathway at this location. Moreover, within ERT stations 219 to 366, bedrock is mostly characterized by moist bedrock (125 ohm-m < resistivities < 900 ohm-m), which is attributed to concentrated run-off flowing along several surface drainage pathways towards the east topographic low (the landfill was constructed this way for run-off control).

Visual analysis of the resistivity pattern of ERT profile 6 also suggests moisture seeped through the subsurface along near vertical seepage pathways (highlighted in blue arrows). Moisture content in the bedrock is the greatest where immediately adjacent to the north toe of the landfill, and gradually decreases with increasing distance to the toe (except in some areas where anthropogenic features are present), indicating there also appears to be a lateral component to seepage, away from the landfill. These findings are consistent with and support the previous interpretations of ERT profiles 1 to 5.

5.4. ERT Profile 6A

At a different time of year, ERT profile 6A (**Figure 11**) was acquired essentially at the same location as ERT profile 6 (along a slightly longer traverse).

ERT profile 6A was acquired in early February. Precipitation and snowmelt in the winter month were limited and as a result, run-off significantly decreased. Subsurface bedrock immediately adjacent to the north toe of the landfill and anthropogenic features is mostly characterized by dry bedrock (resistivities > 900 ohm-m), indicating very little moisture has seeped through the subsurface in these areas.

On the contrary, ERT profile 6 was acquired in early September, run-off increased from significant rainfall in the later summer month. Subsurface bedrock immediately adjacent to the same features (the north toe of the landfill and anthropogenic features) is mostly characterized by moist bedrock (125 ohm-m < resistivities < 900 ohm-m), indicating relatively higher moisture has seeped through the subsurface in these areas.

These findings are consistent with and support the previous interpretations presented in this paper, that the most prominent seepage pathways are a result of stormwater run-off concentrating and seeping downward at the toe of the landfill and by anthropogenic features.

6. Conclusion

Electrical resistivity tomography data were acquired in proximity to a CCR landfill located in southwest Missouri. ERT data were interpreted with the aid of boring control, MASW control and ERT control in the general study area.

Local soil is generally characterized by resistivities less than 125 ohm-m, except

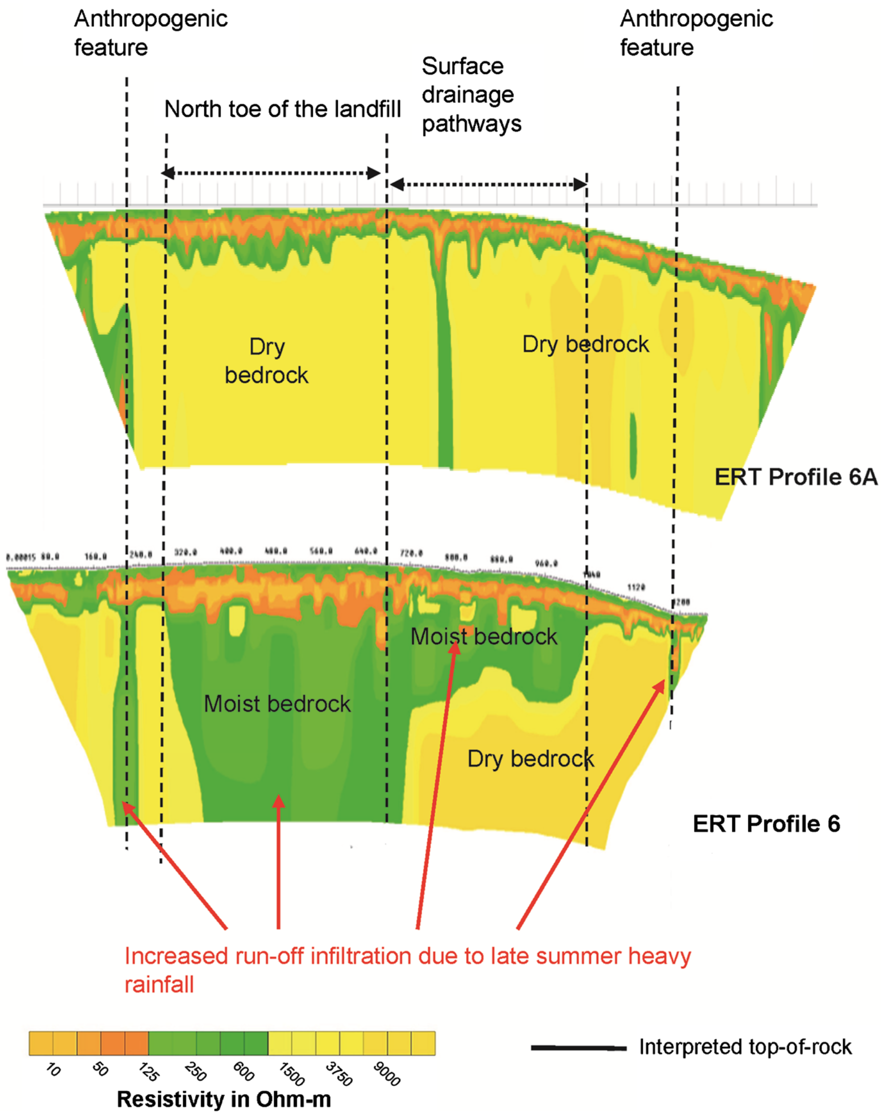

Figure 11. Comparison of interpreted ERT profile 6A (upper) and ERT profile 6 (lower).

in areas where soil is dry. The pre-development residual soil profile is approximately 20 ft (6.096 m) thick. Rock is generally characterized by resistivities greater than 900 ohm-m, except in areas where rock is moist and piped clay may be present. In such areas, rock resistivities can be less than 125 ohm-m. The most prominent seepage pathways locate in the subsurface weathered permeable soil and pervasively fractured upper bedrock, immediately adjacent to the toe of the CCR landfill, and are attributed to stormwater run-off accumulating and seeping downward at the toe. Other prominent seepage pathways are associated with anthropogenic features, such as clay berms, drainage ditches, roadways, and natural drainage pathways. These features cause run-off to accumulate locally and seep into the subsurface.

The overall resistivity of the bedrock decreases with increasing distance to the landfill toe. Additionally, the overall resistivity of the bedrock decreases with increasing distance to anthropogenic features. Seepage at the toe of the landfill tends to percolate vertically into the subsurface, with a lateral component to seepage, away from the landfill toe. Lastly, resistivity of the subsurface varies seasonally with precipitation.

Acknowledgements

Part of the materials contained in this paper was previously published in the first author's Ph.D. dissertation.

Conflicts of Interest

The authors declare no conflicts of interest regarding the publication of this paper.

References

Claerbout, J. F., & Muir, F. (1973). Robust Modeling with Erratic Data. *Geophysics, 38,* 826-844. https://doi.org/10.1190/1.1440378

Degroot-Hedlin, C., & Constable, S. (1990). Occam's Inversion to Generate Smooth, Two-Dimensional Models from Magnetotelluric Data. *Geophysics, 55,* 1613-1624. https://doi.org/10.1190/1.1442813

Kidanu, S. T., Torgashov, E. V., Varnavina, A. V., & Anderson, N. L (2016). ERT-Based Investigation of a Sinkhole in Greene County, Missouri. *AIMS Geosciences, 1,* 99-115. https://doi.org/10.3934/geosci.2016.2.99

Loke, M. H., Acworth, I., & Dahlin, T. (2003). A Comparison of Smooth and Blocky Inversion Methods in 2D Electrical Imaging Surveys. *Exploration Geophysics, 34,* 182-187. https://doi.org/10.1071/EG03182

Loke, M. H. (2018). *Tutorial: 2-D and 3-D Electrical Imaging Surveys* (pp. 31-35). Malaysia: Geotomo Software.

Sasaki, Y. (1992). Resolution of Resistivity Tomography Inferred from Numerical Simulation. *Geophysical Prospecting, 40,* 453-463. https://doi.org/10.1111/j.1365-2478.1992.tb00536.x

Shepard, E. M. (1898). *A Report on Greene County: Missouri*. Geol. Survey, 1st Ser. v. 12, pp. 13-245.

US EPA (2015). *Hazardous and Solid Waste Management System; Disposal of Coal Combustion Residuals from Electric Utilities*. Federal Register.

Vandike, J. E. (1993). *Groundwater Level Data for Missouri: Water Year 1991-1992*. Water Resource Report No. 42, Rolla, MO: Missouri Department of Natural Resources. Division of Geology and Land Survey.

Vandike, J. E., & Sherman, L. D. (1994). *Hydrogeologic Investigation of the Fulbright Area, Greene County, Missouri*. https://dnr.mo.gov/pubs/WR43.pdf

Zhao, R., & Anderson, N. (2018). A Description of Field Setup and Common Issues in 2-D Electrical Resistivity Tomography Data Acquisition. *International Journal of Science and Research, 7,* 1061-1066. https://doi.org/10.21275/ART20193810

Zhao, R. (2018). *Delineation of a Coal Combustion Residue Landfill and Underlying Karst Sub-Surface in Southwest Missouri Using ERT and MASW Surveys*. Doctoral Dissertation, Rolla, MO: Missouri University of Science and Technology. https://scholarsmine.mst.edu/doctoral_dissertations/2857

Zhao, R., Anderson, N., & Sun, J. (2020). Geophysical Investigation of a Solid Waste Disposal Site Using Integrated Electrical Resistivity Tomography and Multichannel Analyses of Surface Waves Methods. *Journal of Geoscience and Environment Protection, 8,* 55-69. https://doi.org/10.4236/gep.2020.83005